

Effects of Conduction on Magneto-Hydrodynamics Mixed Convection Flow in Triangular Enclosures

[1]Muhammad Sajjad Hossain*, [2]M. A. Hoque and [3]Md. Kamruzzaman

[1]Assistant Professor of Mathematics, [2]Lecturer in Mathematics, [3]Lecturer in Physics
Department of Arts and Sciences, Ahsanullah University of Science & Technology (AUST)
Dhaka-1208, Bangladesh.

*Corresponding author's email: msh80_edu@yahoo.com

ABSTRACT

We study the significance of conduction with magneto-hydrodynamics (MHD) mixed convection flow in triangular enclosures. The enclosures consist of one temperature of the left moving wall, which has constant flow speed. A uniform magnetic field is applied in the horizontal direction normal to the moving wall. The results indicate that both the flow and the thermal fields strongly depend on the Hartmann number *Ha*, Prandlt number *Pr* for fixed Reynolds number *Re*, at the convective regimes. It is also observed that, the parameters Prandtl number *Pr* influence on the flow fields and have significant effect on the thermal fields at the convective regimes. According to the results it is found that both the flow and thermal fields inside the enclosures strongly depend on the relevant dimensionless groups. For the purpose of comparison of the effect of MHD on heat transfer, the results in terms of average Nusselt number and average temperature are shown in tabular form.

Keywords: Streamfunction, Isotherms, Triangular Enclosures, MHD

1. INTRODUCTION

Mixed convection is a combination of forced and free convections which is the general case of convection when a flow is determined simultaneously by both an outer forcing system (i.e., outer energy supply to the fluid-streamlined body system) and inner volumetric (mass) forces, viz., by the nonuniform density distribution of a fluid medium in a gravity field. The most vivid manifestation of mixed convection is the motion of the temperature stratified mass of air and water areas of the Earth that the traditionally studied in geophysics. However, mixed convection is found in the systems of much smaller scales, i.e., in many engineering devices. On heating or cooling of channel walls, and at the small velocities of a fluid flow that are characteristic of a laminar flow, mixed convection is almost always realized. Many mathematicians, versed engineers and researchers studied the problems of MHD mixed convection for different types of cavity. Amongst them, Oreper and Szekely (1983) studied the effect of an externally imposed magnetic field on buoyancy driven flow in a rectangular cavity. They found that the presence of a magnetic field can suppress natural convection currents and that the strength of the magnetic field is one of the important factors in determining the quality of the crystal.

Ozoe and Maruo (1987) investigated magnetic and gravitational natural convection of melted silicon two-dimensional numerical computations for the rate of heat transfer. Rudraiah et al. (1995a) investigated the effect of surface tension on buoyancy driven flow of an electrically conducting fluid in a rectangular cavity in the presence of a vertical transverse magnetic field to see how this force damps hydrodynamic movements. At the same time, Rudraiah et al. (1995b) also studied the effect of a magnetic field on free convection in a rectangular enclosure. The problem of unsteady laminar combined forced and free convection flow and heat transfer of an electrically conducting and heat generating or absorbing fluid in a vertical liddriven cavity in the presence of a magnetic field was formulated by Chamkha (2002).Recently, Rahman et al. (2009a) studied the effect of a heat conducting horizontal circular cylinder on MHD mixed convection in a lid-driven cavity along with Joule Heating. The author considered the cavity consists of adiabatic horizontal walls and differentially heated vertical walls, but it also contains a heat conducting horizontal circular cylinder located somewhere inside the cavity. The results indicated that both the flow and thermal fields strongly depend on the size and locations of the inner cylinder, but the thermal conductivity of the cylinder has significant effect only on the thermal field. Rahman et al.(2009b)

investigated the effect on magnetohydrodynamic (MHD) mixed convection around a heat conducting Horizontal circular cylinder placed at the center of a rectangular cavity along with joule heating. They observed that the streamlines, isotherms, average Nusselt number, average fluid temperature and dimensionless temperature at the cylinder center strongly depend on the Richardson number, Hartmann number and the cavity aspect ratio. Very recently, Rahman et al. (2010) made numerical investigation on the effect of magneto hydrodynamic (MHD) mixed convection flow in a vertical lid driven square enclosure including a heat conducting horizontal circular cylinder with Joule heating. The author found that the Hartmann number, Reynolds number and Richardson number have strong influence on the streamlines and isotherms.

To the best of our knowledge in the light of the above literatures, it has been pointed out that no work has been paid on MHD mixed convection inside a triangular enclosure yet.The aim proposed research is to investigate the effects of Magneto hydrodynamic (MHD) mixed convection flow in a triangular enclosures. Results will be presented for different non-dimensional governing and physical parameters in terms of streamlines, isotherms, heat transfer rate as well as the average temperature of the fluid in the enclosures.

2. PHYSICAL MODEL

The physical model considered here is shown in Fig. 1, along with the important geometric parameters. The heat transfer and the fluid flow in a two-dimensional triangular enclosure with MHD flow whose left wall and bottom wall are subjected to cold *Tc* and hot *Th* temperatures respectively while the inclined walls are kept adiabatic. The fluid was assumed with Prandtl number (*Pr* = 0.71, 2.0, 3.0, 6.0), Reynolds number *(Re* = 50), Hartmann number (*Ha* = 5-50) and Newtonian, and the fluid flow is considered to be laminar. The properties of the fluid were assumed to be constant.

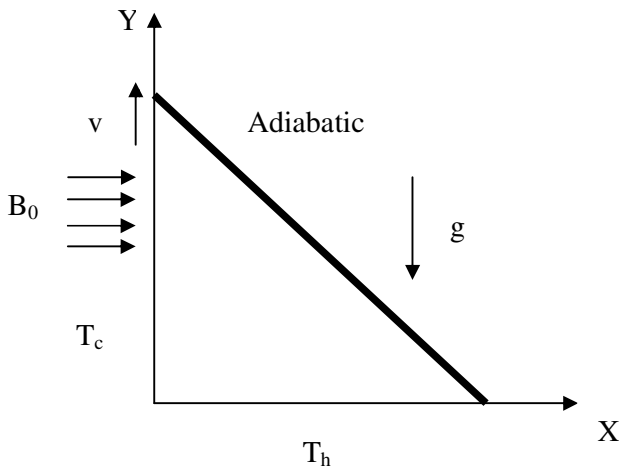

Figure 1: Schematic diagram of the physical system

3. MATHEMATICAL FORMULATION

The fundamental laws used to solve the fluid flow and heat transfer problems are the conservation of mass (continuity equations), conservation of momentums (momentum equations), and conservation of energy (energy equations), which constitute a set of coupled, nonlinear, partial differential equations. For laminar incompressible thermal flow, the buoyancy force is included here as a body force in the *v*-momentum equation. The governing equations for the two-dimensional steady flow after invoking the Boussinesq approximation and neglecting radiation and viscous dissipation can be expressed as:

$$\frac{\partial U}{\partial X}+\frac{\partial V}{\partial Y}=0 \tag{1}$$

$$U\frac{\partial U}{\partial X}+V\frac{\partial U}{\partial Y}=-\frac{\partial P}{\partial X}+\frac{1}{Re}\left(\frac{\partial^2 U}{\partial X^2}+\frac{\partial^2 U}{\partial Y^2}\right) \tag{2}$$

$$U\frac{\partial U}{\partial X}+V\frac{\partial U}{\partial Y}=-\frac{\partial P}{\partial Y}+\frac{1}{\mathrm{Re}}\left(\frac{\partial^2 V}{\partial X^2}+\frac{\partial^2 V}{\partial Y^2}\right)+Ra\,\mathrm{Pr}\,\theta-\frac{Ha^2}{\mathrm{Re}}V \quad (3)$$

$$U\frac{\partial \theta}{\partial X}+V\frac{\partial \theta}{\partial Y}=\frac{1}{Re\,Pr}\left(\frac{\partial^2 \theta}{\partial X^2}+\frac{\partial^2 \theta}{\partial Y^2}\right) \quad (4)$$

The dimensionless parameters appearing in the equations (4.5) through (4.8) are Reynolds number, $\mathrm{Re}=\frac{u_i L}{\nu}$, Grashof number, $Gr=\frac{\beta g\Delta T L^3}{\nu^2}$, Prandtl number, $\mathrm{Pr}=\frac{\nu}{\alpha}$, Hartmann number, $Ha^2=\frac{\sigma B_0^2 L^2}{\mu}$, Rayleigh number, $Ra=Gr\times\mathrm{Pr}$, temperature difference, $\Delta T=T_h-T_c$ and thermal diffusivity, $\alpha=\frac{\kappa}{\rho C_p}$, where non-dimensional variables are as follows:

$$X=\frac{x}{L},Y=\frac{y}{L},U=\frac{u}{v_0},V=\frac{v}{v_0},P=\frac{p}{\rho v_0^2},\theta=\frac{(T-T_c)}{(T_h-T_c)}$$

Where *X* and *Y* are the coordinates varying along horizontal and vertical directions, respectively, *U* and *V* are the velocity components in the *X* and *Y* directions, respectively, θ is the dimensionless temperature and *P* is the dimensionless pressure.

The appropriate dimensionless boundary conditions for the above equations () can be written as:

At the left vertical wall: *U*=0, *V*=1, $\theta=0$

At the bottom wall: *U*=0, *V*=0, $\theta=1$

At the inclined wall: *U*=0, *V*=0, $\frac{\partial\theta}{\partial N}=0$

Where *N* is the non-dimensional distances either along *X* or *Y* direction acting normal to the surface and *K* is the dimensionless thermal conductivity.

According to Singh and Sharif (2003), the average Nusselt number at the heated wall of the enclosures based on the non-dimensional variables may be expressed as $Nu=\int_0^1\left(\frac{\partial\theta}{\partial Y}\right)_{y=0}dX$ and the bulk average temperature defined as $\theta_{av}=\int\theta\,d\overline{V}/\overline{V}$, where $\overline{V}$ is the enclosures volume.

4. FINITE ELEMENT TECHNIQUE

The Galerkin finite element method (1973, 1999) is used to solve the non-dimensionalgoverning equations along with boundary conditions for the considered problem. The equation of continuity has been used as a constraint due to mass conservation and thisrestriction may be used to find the pressure distribution. The basic unknowns for the above differential equations are the velocity components *U*, *V*, the temperature θ and the pressure *P*. The velocity components, the temperature distributions and linear interpolation for the pressure distribution according to their highest derivative orders in the differential eqs. (1) - (4) are as follows:

$$U(X,\ Y)=N_\alpha U_\alpha,\quad V(X,\ Y)=N_\alpha V_\alpha,\quad \theta(X,Y)=N_\alpha\ \theta_\alpha,\quad P(X,\ Y)=H_\lambda P_\lambda$$

where α = 1, 2, … …, 6; λ= 1, 2, 3; N_α are the element interpolation functions for the velocity components and the temperature, and H_λ are the element interpolation functions for the pressure.
To derive the finite element equations, the method of weighted residuals finite-element formulation is applied to the equations (1) – (4) as

$$\int_A N_\alpha \left(\frac{\partial U}{\partial X} + \frac{\partial V}{\partial Y} \right) dA = 0 \tag{5}$$

$$\int_A N_\alpha \left(U \frac{\partial U}{\partial X} + V \frac{\partial U}{\partial Y} \right) dA = -\int_A H_\lambda \left(\frac{\partial P}{\partial X} \right) dA + \frac{1}{Re} \int_A N_\alpha \left(\frac{\partial^2 U}{\partial X^2} + \frac{\partial^2 U}{\partial Y^2} \right) dA \tag{6}$$

$$\int_A N_\alpha (U \frac{\partial V}{\partial X} + V \frac{\partial V}{\partial Y}) dA = -\int_A H_\lambda (\frac{\partial P}{\partial Y}) dA + \frac{1}{\mathrm{Re}} \int_A N_\alpha (\frac{\partial^2 V}{\partial X^2} + \frac{\partial^2 V}{\partial Y^2}) dA + Ra \,\mathrm{Pr} \int_A N_\alpha \theta dA - \frac{Ha^2}{\mathrm{Re}} \int_A N_\alpha V dA \tag{7}$$

$$\int_A N_\alpha \left(U \frac{\partial \theta}{\partial X} + V \frac{\partial \theta}{\partial Y} \right) dA = \frac{1}{Re\, Pr} \int_A N_\alpha \left(\frac{\partial^2 \theta}{\partial X^2} + \frac{\partial^2 \theta}{\partial Y^2} \right) dA \tag{8}$$

So, the coefficients in element matrices are in the form of the integrals over the element area as,

$$K_{\alpha\beta^x} = \int_A N_\alpha N_{\beta,x} dA, \quad K_{\alpha\beta^y} = \int_A N_\alpha N_{\beta,y} dA, \quad K_{\alpha\beta\gamma^x} = \int_A N_\alpha N_\beta N_{\gamma,x} dA$$

$$K_{\alpha\beta\gamma^y} = \int_A N_\alpha N_\beta N_{\gamma,y} dA, \quad K_{\alpha\beta} = \int_A N_\alpha N_\beta dA, \quad S_{\alpha\beta^{xx}} = \int_A N_{\alpha,x} N_{\beta,x} dA$$

$$S_{\alpha\beta^{yy}} = \int_A N_{\alpha,y} N_{\beta,y} dA, \quad M_{\alpha\mu^x} = \int_A H_\alpha H_{\mu,x} dA, \quad M_{\alpha\mu^y} = \int_A H_\alpha H_{\mu,y} dA$$

$$Q_{\alpha^\mu} = \int_{S_0} N_\alpha S_x dS_0, \quad Q_{\alpha^v} = \int_{S_0} N_\alpha S_y dS_0, \quad Q_{\alpha\theta} = \int_{S_w} N_\alpha \, q_{1w} dS_w$$

$$Q_{\alpha\theta_s} = \int_{S_w} N_\alpha \, q_{2w} dS_w$$

Using reduced integration technique of Reddy (1985) and Newton-Raphson iteration technique by first writing the unbalanced values from the set of the finite element equations, the nonlinear algebraic Eqs. (5) - (8) so obtained are modified by imposition of boundary conditions. These modified nonlinear equations are transferred into linear algebraic equations by using Newton's method. Finally, these linear equations are solved by using Triangular Factorization method.

5. MESH GENERATION

The present numerical technique will discretize the computational domain into unstructured triangles by Delaunay Triangular method. The Delaunay triangulation is a geometric structure that has enjoyed great popularity in mesh generation since the mesh generation was in its infancy. In two dimensions, the Delaunay triangulation of a vertex set maximizes the minimum angle among all possible triangulations of that vertex set.

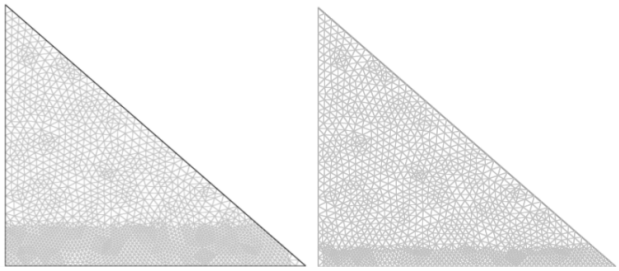

Figure 2: Current mesh structure of elements for triangular enclosures.

6. GRID INDEPENDENCE TEST

A grid refinement study is performed for a square open enclosures to obtain grid refinement solution with $Pr = 0.71$, $Re = 50$, Ha = 20 and $Ra = 10^4$. Figure 3 shows the convergence of the average Nusselt number, Nu_{av} at the heated surface with grid refinement. It is observed that grid independence is achieved with 13398 elements where there is insignificant change in Nu with further increase of mesh elements.

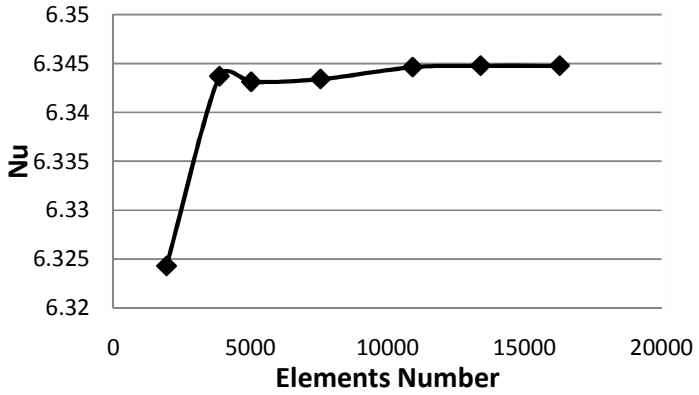

Figure 3: Convergence of average Nusselt number with grid refinement for Pr = 0.71, Re= 50, Ha=20 and $Ra = 10^4$.

7. CODE VALIDATION

The computed average Nusselt numbers for the constant surface temperature and different Rayleigh Numbers are tabulated in Table 1 for numerical code validation against the numerical results of Basak et al. (2007), for pure natural convection with Pr = 0.71 in a triangular enclosures. It is seen the present computation and those of Basak et al.(2007), are good agreement.

Ra	Nu_{av}	
	Present work	Basak et al. (2007)
10^3	5.49	5.40
10^4	5.77	5.56
10^5	7.08	7.54

Table 1: Comparison between Basak et.al.(2007) and present work

8. RESULTS AND DISCUSSION

The MHD mixed convection flow and temperature fields as well as heat transfer rates and bulk temperature inside the triangular enclosures has been numerically investigated. The MHD mixed convection phenomenon inside the enclosure is strongly influenced by governing as well as physical parameters, namely and Hartman number Ha, Reynolds number Re, Prandtl number Pr, Rayleigh number Ra. As the nature of flow and thermo physical properties of fluid strongly influenced on the heat transfer rate, and the numerical computation were performed for a range of Ha, Re and Pr (Ha =5-50, Re = 50, Pr = 0.71-6). In addition, for each value of mentioned parameters, computations are performed at $Ra = 5 \times 10^3$ that focuses on pure mixed convection. Moreover, the results of this study are presented in terms of streamlines and isotherms. Furthermore, the heat transfer effectiveness of the enclosure is displayed in terms of average Nusselt number Nu and the dimensionless average bulk temperature θ_{av}.

8.1 EFFECTS OF HARTMAN NUMBER

The special effects of Hartmann number Ha on the flow and thermal fields at Ra= $1e^3$ to $1e^4$ is illustrate in Figure 4 - 7, while Pr = 0.71 and Re = 50 are kept fixed. In this folder, the size of the counter clockwise vortex also decreases sharply with increasing of Ha. This is because application of a slanting magnetic field has the propensity to slow down the movement of the buoyancy induced flow in the enclosures. The effects of Hartmann number Ha on isotherms are shown in the Figure 4 – 7 while Re = 50 and Pr = 0.71 are kept fixed. It is observed that the higher values isotherms are more tightened at the vicinity of the heated wall of the enclosures for the considered value of Ra. A similar trend is found for the higher values of Ha. From this figure it can easily be seen that isotherms are almost parallel at the vicinity of the bottom

horizontal hot wall but it changes to parabolic shape with the increasing distance from inclined wall for the highest value of *Ha* (=20.0) at *Pr* = 0.71, indicating that most of the heat transfer process is carried out by conduction. In addition, it is noticed that the isothermal layer near the heated surface becomes slightly thin with the decreasing *Ha*. However in the remaining area near the left wall of the enclosures, the temperature gradients are small in order to mechanically driven circulations.

The effects of *Ha* on average Nusselt number *Nu* at the heated surface and average bulk temperature θ_{av} in the enclosures is illustrated in Fig. 8 & 9 with *Re* =50 and *Pr* =0.71. From this figure, it is found that the average Nusselt number *Nu* decreases with increasing *Pr*. It is to be highlighted that the highest heat transfer rate occurs for the lowest values of *Ha* (= 5). The average bulk temperature of the fluid in the enclosures is high for higher values of *Ha* (10 - 50). It is to be mentioned here that the highest average temperature is documented for the higher value of *Ha* in the free convection dominated region.

Table 2: Average Nusselt numbers for different Hartmann number while *Ha* = 5, 10, 20 and 50, *Re*=50 and *Pr*=0.71.

Nu_{av}			
Ha	$Ra=10^3$	$Ra=5\times10^3$	$Ra=10^4$
5	4.38836694	6.434903	5.764501
10	4.36317068	6.413537	5.805674
20	4.26278628	6.331658	5.913316
50	3.79764503	5.890227	5.878074

Table 3: Average bulk temperature for different Hartmann number while *Ha*= 5, 10, 20 and 50, *Re*=50 and *Pr*=0.71.

θ_{av}			
Ha	$Ra=10^3$	$Ra=5\times10^3$	$Ra=10^4$
5	0.593528	0.566768	0.57386
10	0.593913	0.567008	0.570757
20	0.598198	0.568812	0.561785
50	0.633216	0.585029	0.533999

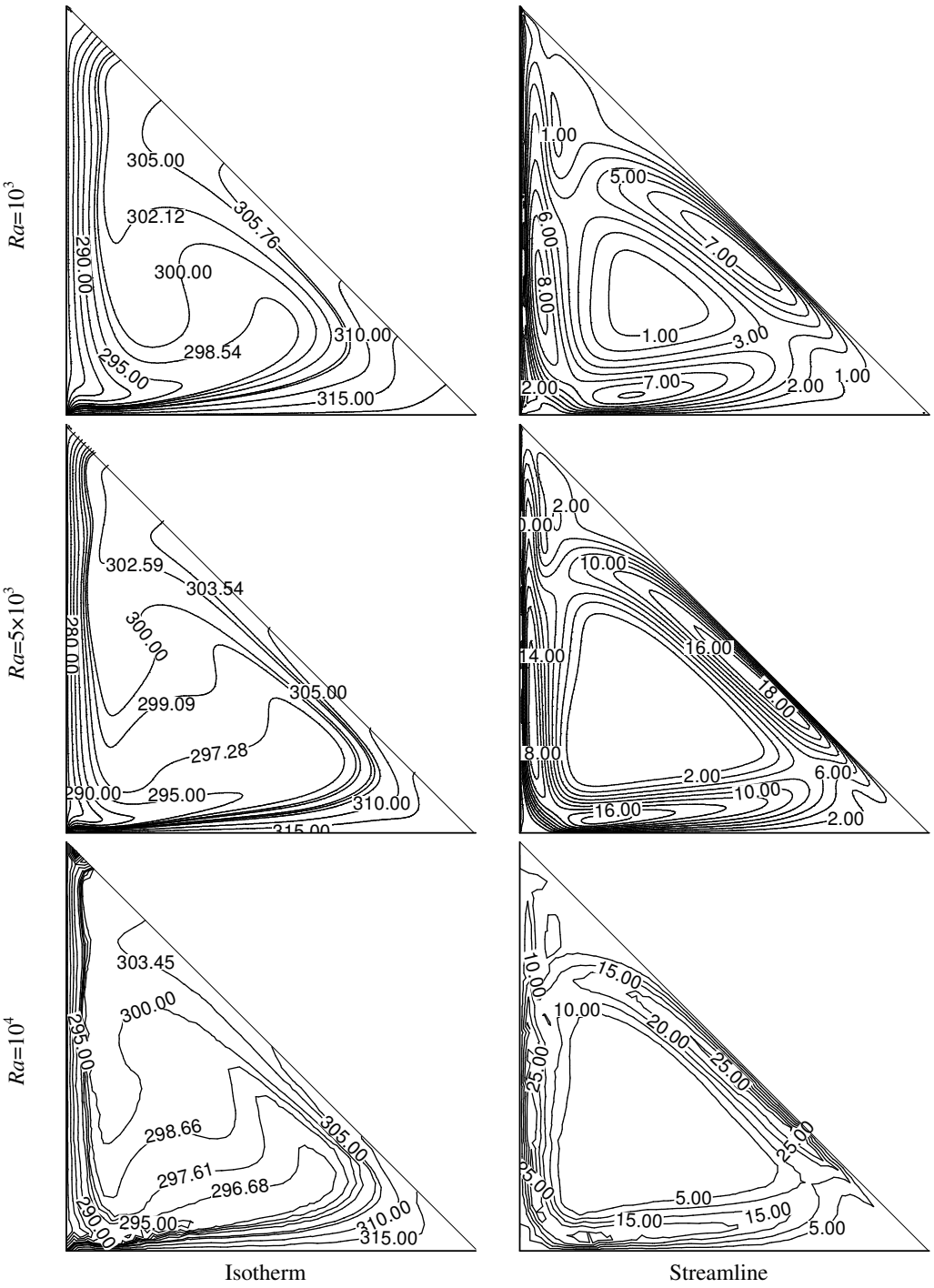

Fig 4: Isotherms and streamlines patterns for Re = 50, Pr = 0.71 and Ha = 5

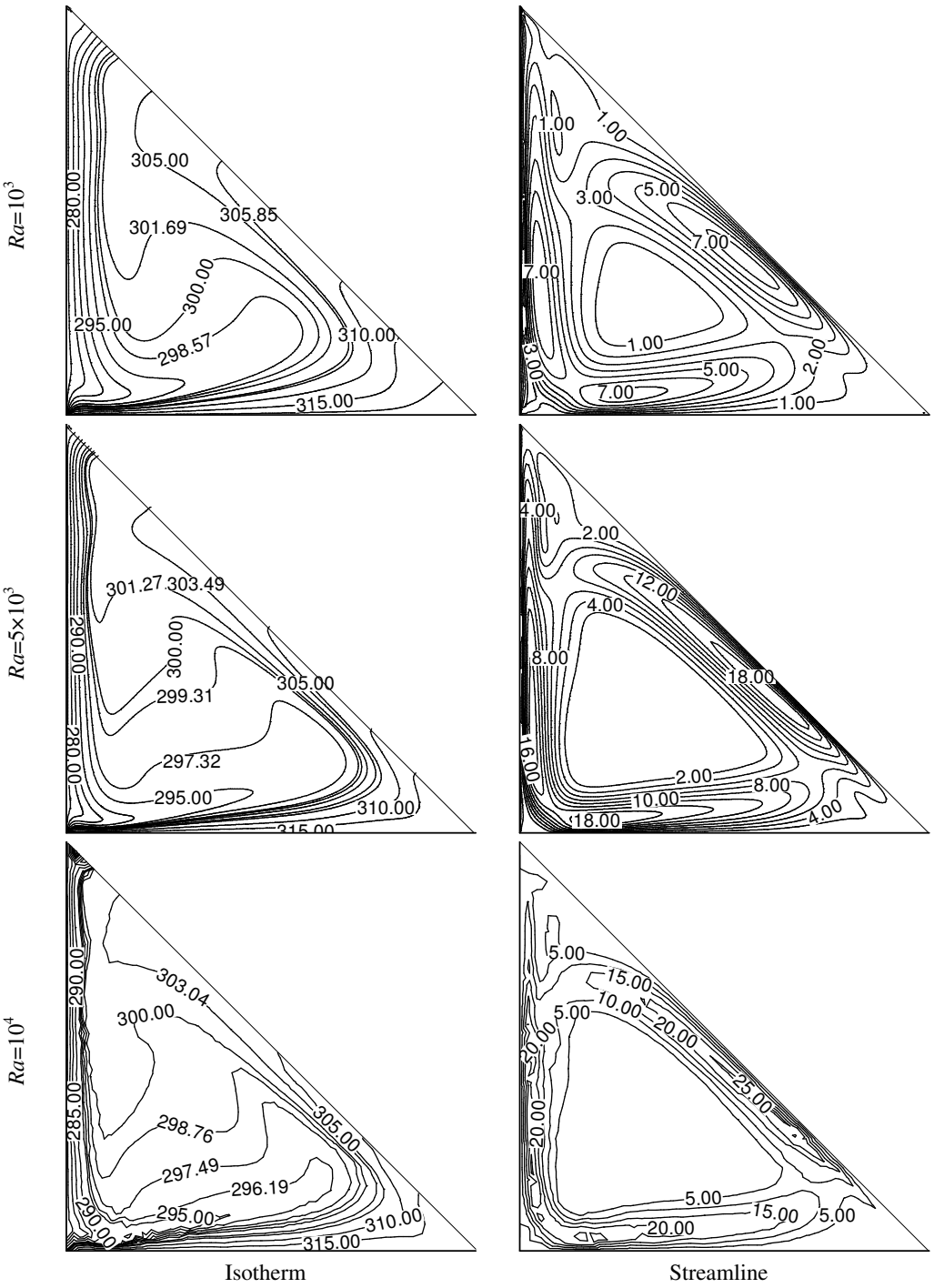

Fig 5: Isotherms and streamlines patterns for Re = 50, Pr = 0.71 *and* Ha = 10

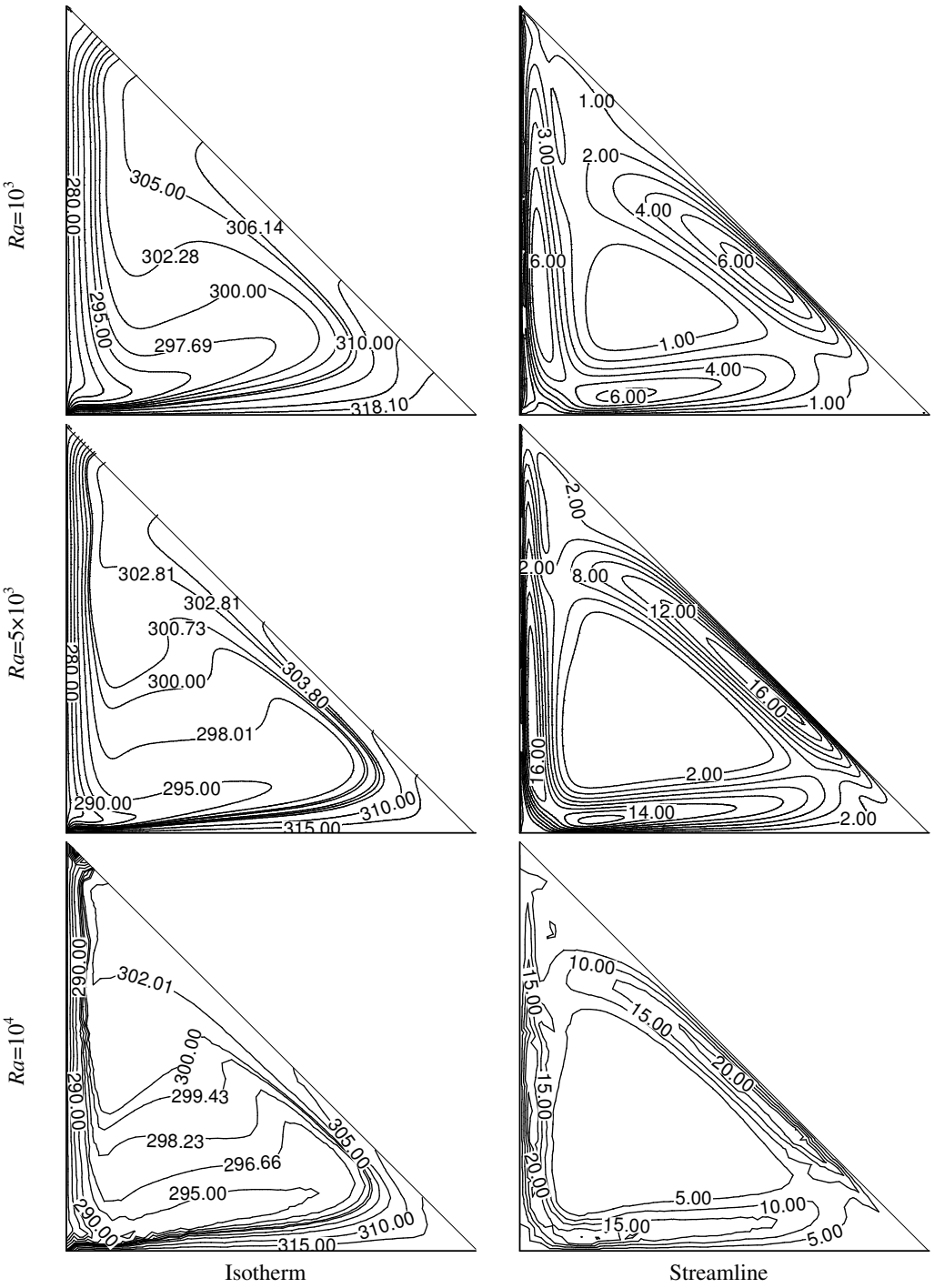

Fig 6: Isotherms and streamlines patterns for Re = 50, Pr = 0.71 and Ha = 20

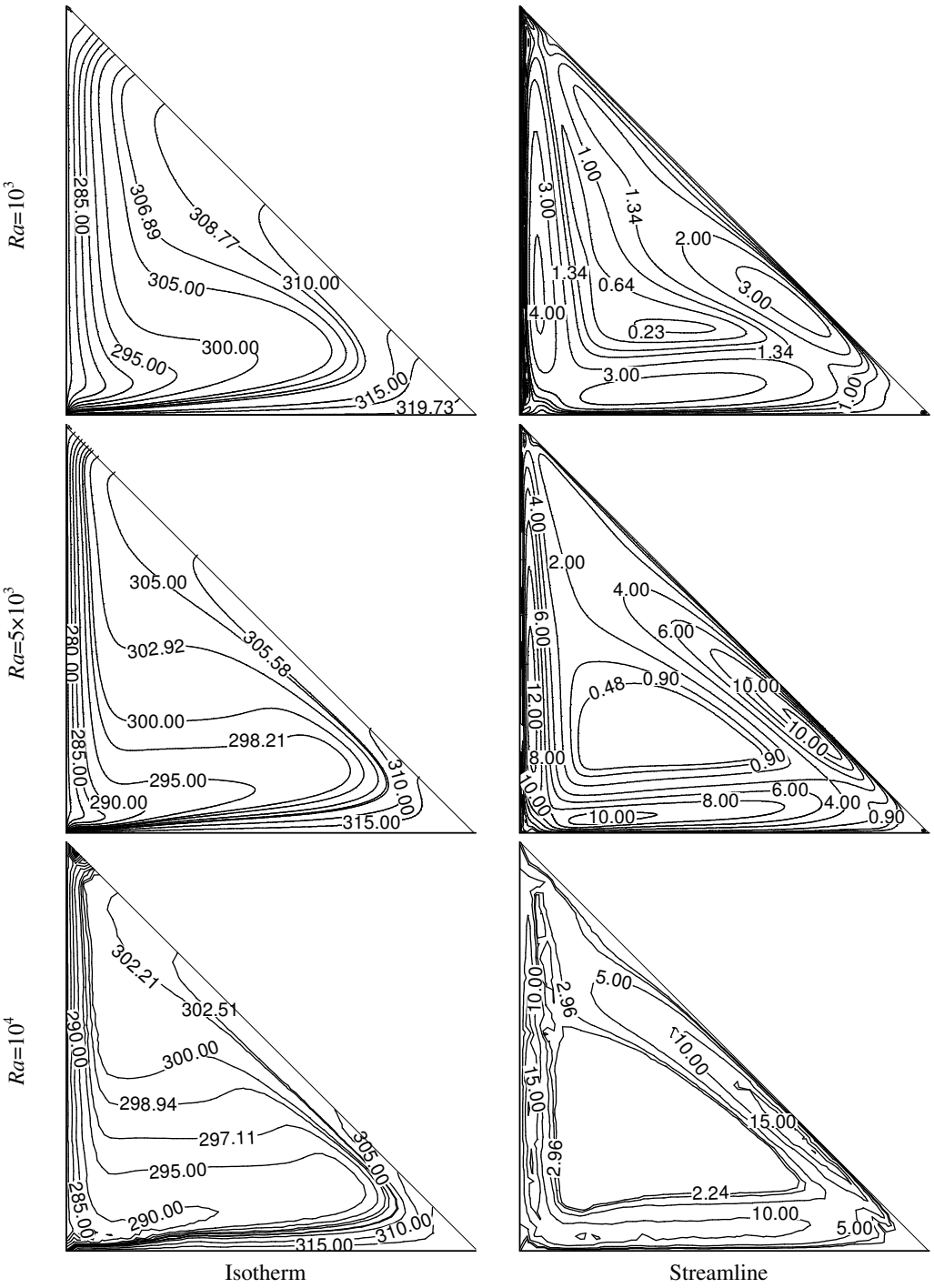

Fig 7: Isotherms and streamlines patterns for Re = 50, Pr = 0.71 and Ha = 50

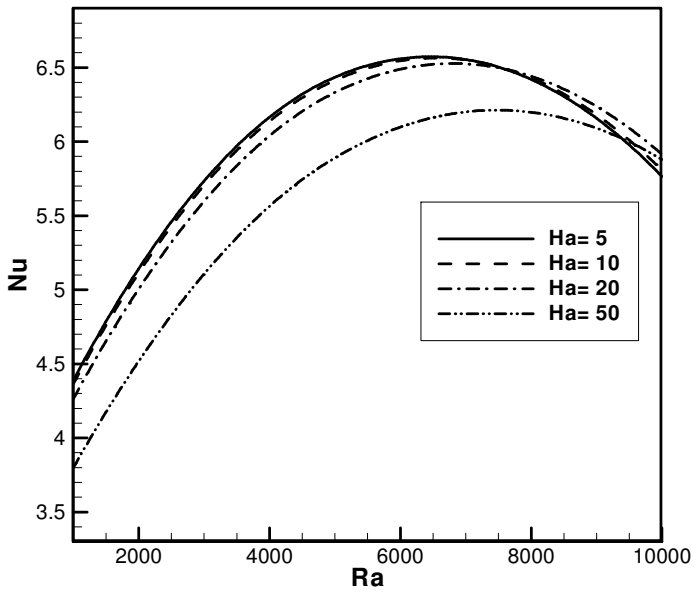

Fig. 8: Effect of average Nusselt number and Rayleigh number while Pr = 0.71 and Re = 50.

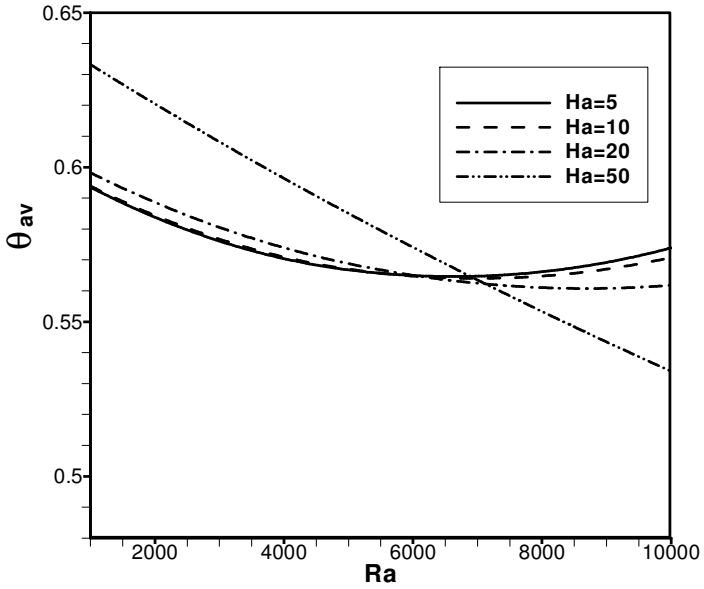

Fig. 9: Effect of average bulk temperature and Rayleigh number while Pr = 0.71and Re = 50.

8.2 EFFECTS OF PRANDLT NUMBER

The property of Prandtl number on flow fields for the considered *Ra* is depicted in Fig.10 - 13, while *Re* = 50 and *Ha* = 20 are kept fixed. Now, from the figure, it is seen that a small vortex is formed at the center of the enclosures. It is evident that the size of the vortex is increased with the increasing value of *Pr*. The influence of Prandtl number *Pr* on thermal fields for the selected value of *Ra* is displayed in Fig.12 for *Re* = 50 and *Ha* = 20. As expected, the thermal boundary layer decreases in thickness as *Pr* increases. This is reflected by the denser deserting of isotherms close to the heated wall and cooled wall as *Pr* increases. The spread of isotherms at low values of *Pr* is due to a strong stream wise conduction that decreases the stream wise temperature gradient in the field. At the increase of *Pr* the isotherms become linear in the enclosures and impenetrable to respective wall. From the Fig. 13, it can easily be seen that the isotherms for different values of *Pr* at $Ra = 10^4$ are clustered near the heated horizontal wall and cooled vertical heated surface of the enclosure, indicating steep temperature gradient along the vertical direction in this region. Besides, the thermal layer near the heated wall becomes thinner moderately with increasing *Pr*.

The effects of Prandtl number on average Nusselt number *Nu* at the heated surface and average bulk temperature θ_{av} in the enclosures are illustrated in Fig. 14 & 15 with *Re* = 50 and *Ha* = 20. From this figure, it is found that the average Nusselt number *Nu* goes up penetratingly with increasing *Pr*. It is to be highlighted that the highest heat transfer rate occurs for the highest values of *Pr* (= 6). The average bulk temperature of the fluid in the enclosures declines very mildly for higher values of *Pr* (0.71- 6.0). But for the lower values of *Pr*, the average bulk temperature is linear. It is to be mentioned here that the highest average temperature is documented for the lower value of *Pr* (= 0.71) in the free convection dominated region.

Table 4: Average Nusselt numbers for different Prandtl number while *Pr* = 0.71, 2.0, 3.0 and 6.0, *Re*=50 and *Ha=20.*

	Nu_{av}		
Pr	$Ra=10^3$	$Ra=5\times10^3$	$Ra=10^4$
0.71	4.262786	6.331658	7.510701
2.0	4.998317	7.454621	8.857028
3.0	6.807629	10.118253	12.023071
6.0	8.111548	11.920293	13.940204

Table 5: Average bulk temperature for different Prandtl number while *Pr* = 0.71, 2.0, 3.0 and 6.0, *Re*=50 and *Ha=20.*

	θ_{av}		
Pr	$Ra=10^3$	$Ra=5\times10^3$	$Ra=10^4$
0.71	0.598198	0.568812	0.558697
2.0	0.584269	0.550002	0.538424
3.0	0.547777	0.504842	0.490760
6.0	0.524512	0.475957	0.459601

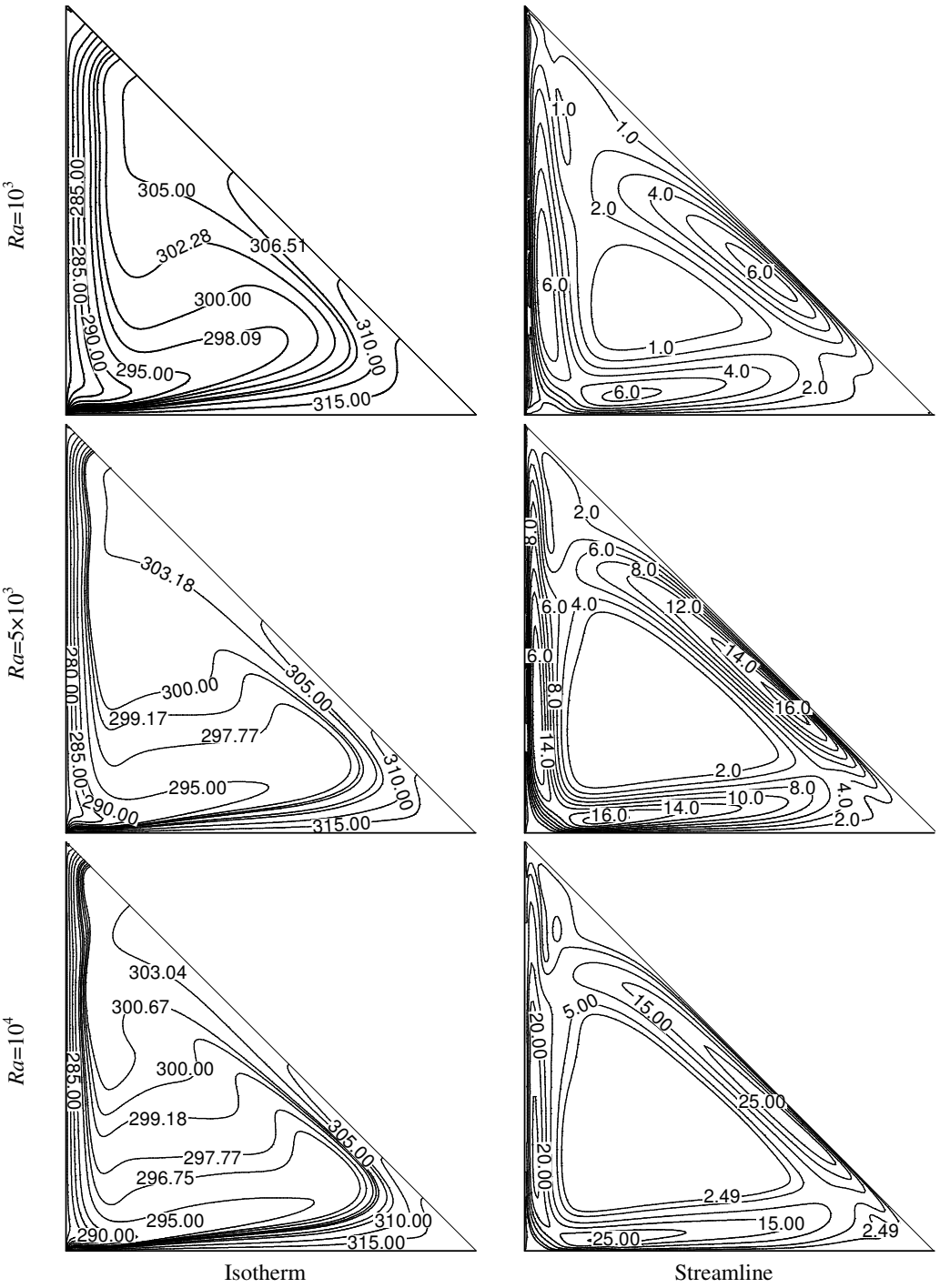

Fig 10: Isotherms and streamlines patterns for Re = 50, Pr = 0.71 and Ha = 20

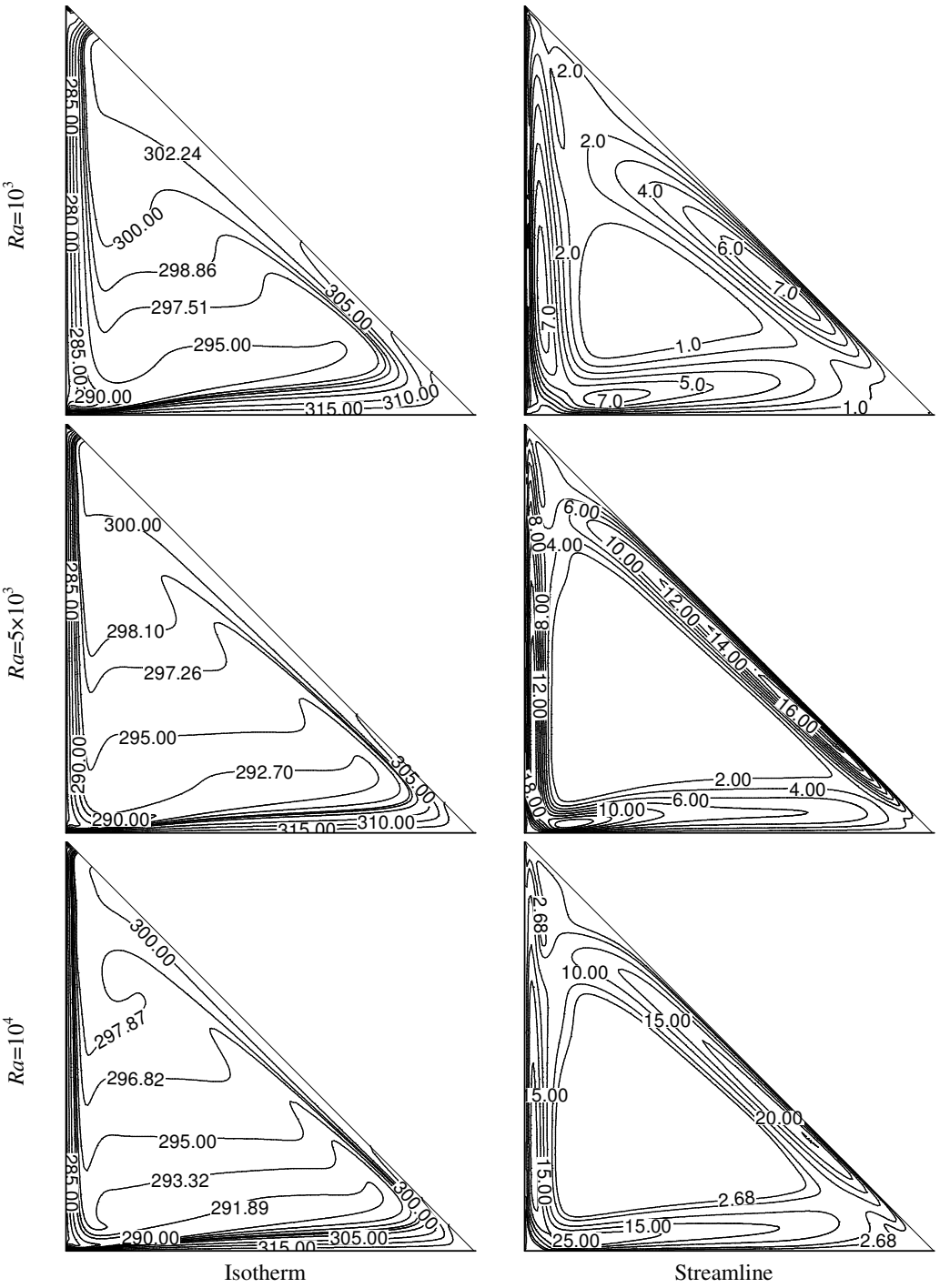

Fig 11: Isotherms and streamlines patterns for Re = 50, Pr = 2.0 and Ha = 20

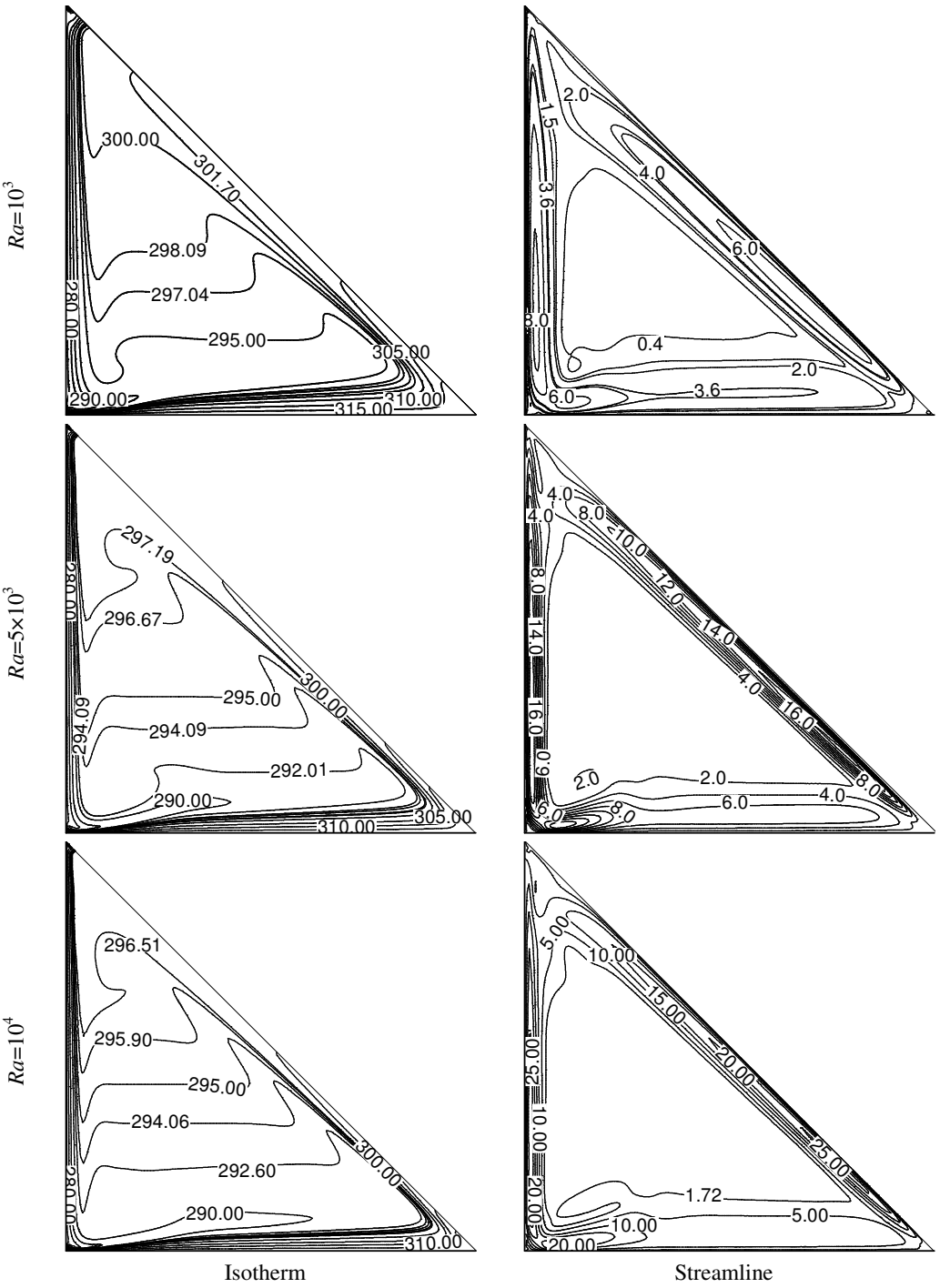

Fig 12: Isotherms and streamlines patterns for Re = 50, Pr = 3.0 and Ha = 20

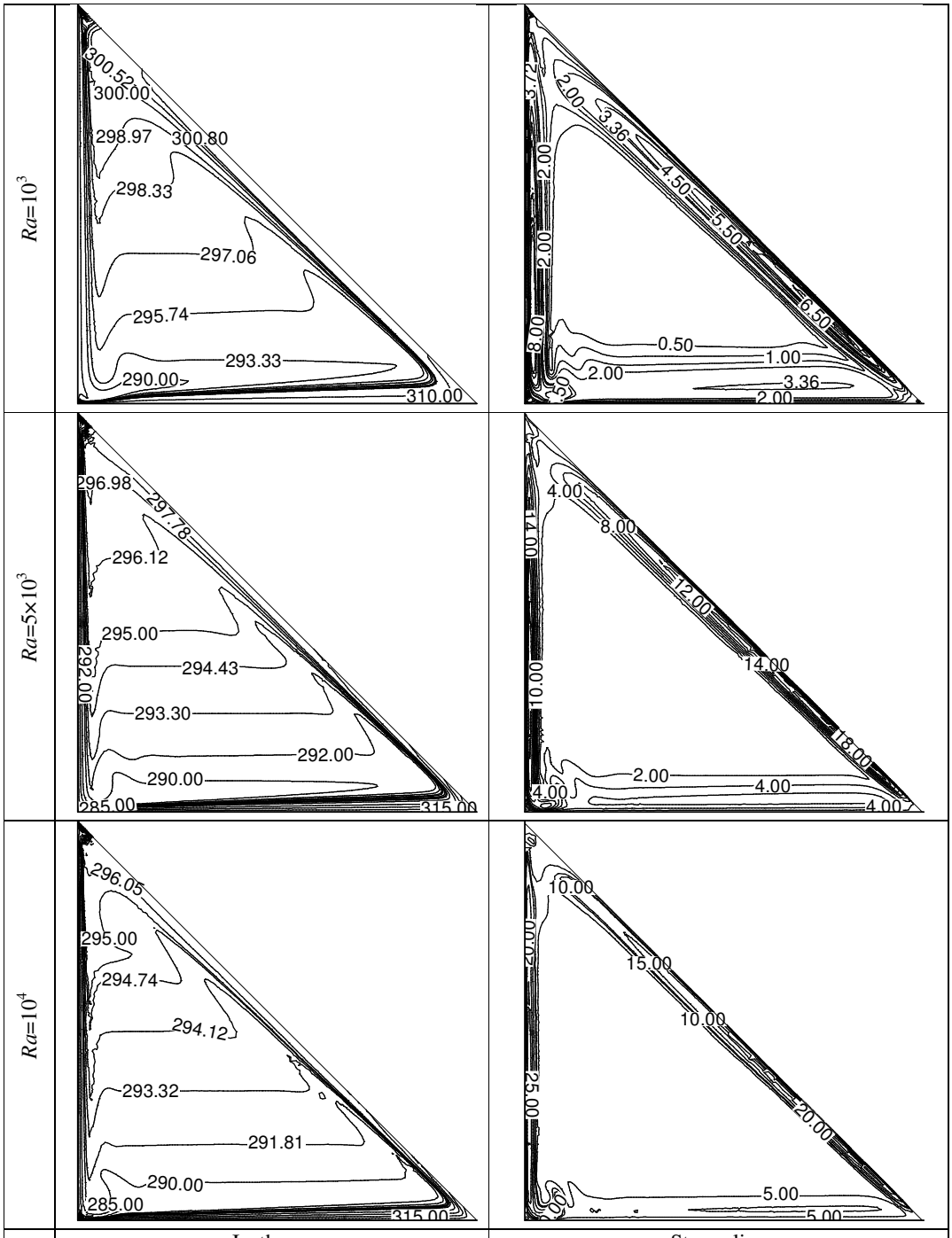

Fig 13: Isotherms and streamlines patterns for Re = 50, Pr = 6.0 and Ha = 20

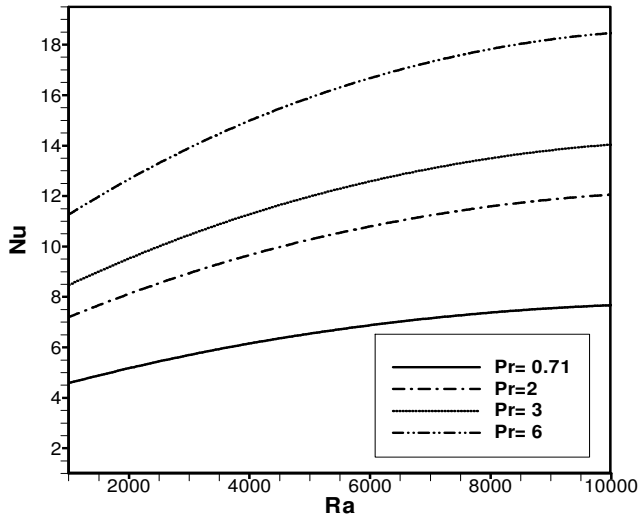

Fig.14: Effect of average Nusselt number and Rayleigh number while *Re* = 50 and *Ha* = 20

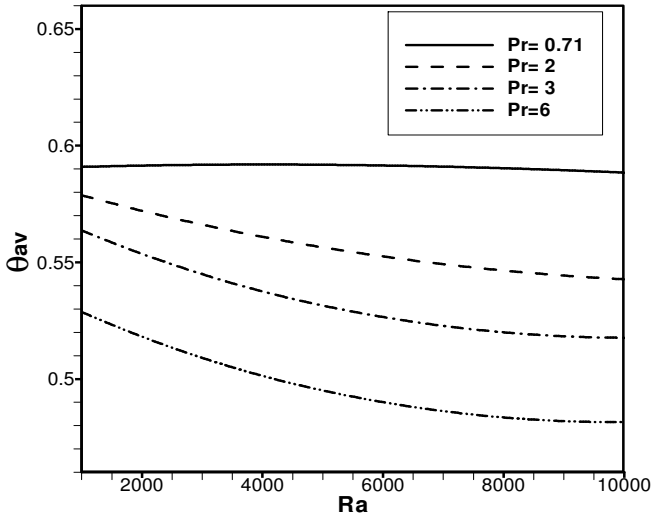

Fig. 15: Effect of average bulk temperature and Rayleigh number while *Re* = 50 and *Ha*=20.

9. CONCLUSIONS

Two-dimensional laminar steady state MHD mixed convection flow in triangular enclosures with the bottom wall at iso-heat flux has been studied numerically. Numerical results have been shown by considering Prandtl numbers of 0.71, 2.00, 3.0 and 6.00, Hartman numbers of 5, 10, 20 and 50, also Rayleigh numbers of 10^3 to 10^4 keeping fixed Reynolds number 50, where the stream line of flow and thermal fields as well as characteristics of heat transfer process particularly its expansion has been evaluated. The results of the numerical analysis lead to the following conclusions:

- The MHD has significant effect on the flow and thermal distributions in the triangular enclosures. The average Nusselt number (*Nu*) at the hot wall is the highest for the *Pr* = 6.0 when Rayleigh number 10^4, whereas the lowest heat transfer rate for the *Ha* = 50 when Rayleigh number 10^3. Moreover, the average Nusselt number with MHD effect is considered higher than those obtained without MHD effect for different value of *Pr* number. However, the average bulk temperature at the hot wall is the lowest for the *Pr* = 6.0 when Rayleigh number 10^4, whereas the highest rate for the *Ha* = 50 when Rayleigh number 10^3
- The heat transfer rate increases steadily with the increase of *Ra* due to increasing of *Ra* number refers that the fluid flow switch from conductive to convective heat transfer. The bulk Temperature decreases smoothly with the increase of *Ra* because at constant conductivity bulk temperature is inversely proportional to the *Nu* (Average Heat Transfer rate).
- The heat transfer rate augments with the increase of *Ra* because when *Pr* number increases, the convective heat transfer is dominated inside the flow field. The bulk Temperature remains linear at *Pr* = 0.71 because low *Pr* number conduction heat transfer dominates in the enclosures. But higher *Pr* bulk temperature decreases as conduction turns into convection.
- With the increase of *Ha* number electromagnetic conduction increases that slow down the heat transfer rate though it increases at forced convection dominated region for a while but fall steadily in mixed convection dominated region.

NOMENCLATURE

θ_{av}	Average temperature
B_0	Magnetic Induction
C_p	Specific heat at constant pressure (J/kg K)
G	Gravitational acceleration (m/s^2)
Gr	Grashof number
H	Convective heat transfer coefficient (W/m^2 K)
k	Thermal conductivity of fluid(W/m K)
K	Tthermal conductivity ratio fluid
N	non-dimensional distance
Nu	Average Nusselt number
Nu_{local}	Local Nusselt number
P	Non-dimensional pressure
p	pressure
Pr	Prandtl number
Ra	Rayleigh number
Re	Reynolds number
T	Non-dimensional temperature
U	Dimensionless horizontal velocity
u	velocity in x-direction (m/s)
V	dimensionless vertical velocity
v	velocity in y-direction (m/s)
V_0	Lid velocity
x, y	Cartesian coordinates
X, Y	dimensionless Cartesian coordinates

Greek symbols

β	Coefficient of thermal expansion (K^{-1})
ρ	Density of the fluid (kg/m^3)
α	Thermal diffusivity (m^2/s)
Δθ	Temperature difference
θ	Fluid temperature
μ	Dynamic viscosity of the fluid (Pa s)
ν	Kinematic viscosity of the fluid (m^2/s)
σ	Fluid electrical conductivity(Ω^{-1}m^{-1})

ACKNOWLEDGEMENTS

We would like to express our gratitude to the Department of Arts and Sciences, Ahsanullah University of Science and Technology (AUST), Dhaka, Bangladesh for providing computing facility during this work.

REFERENCES

Chamkha, A. J. (2002). *Hydromagnetic combined convection flow in a vertical lid-driven enclosures with internal heat generation or absorption*, Numer. Heat Transfer, Part A, Vol. 41, pp. 529-546.

Dechaumphai P. (1999). *Finite Element Method in Engineering*, 2nd ed. (Chulalongkorn Univ. Press, Bangkok,).

Oreper, G. M., Szekely, J. (1983). *The effect of an externally imposed magnetic field on buoyancy driven flow in a rectangular enclosures*, J. of Crystal Growth, Vol. 64, pp. 505-515.

Ozoe, H., and Maruo, M. (1987), *Magnetic and gravitational natural convection of melted silicon-two dimensional numerical computations for the rate of heat transfer*, JSME, Vol. 30, pp. 774-784.

Rahman, M. M., Alim, M. A. (2010). *MHD mixed convection flow in a vertical lid-driven square enclosure including a heat conducting horizontal circular cylinder with Joule heating*, Nonlinear Analysis: Modeling and Control, Vol. 15(2), pp. 199-211.

Rahman, M. M., Alim, M. A., Chowdhury, M. K. (2009b), *Megnetohydrodynamic mixed convection around a heat conducting horizontal circular cylinder in a rectangular liddriven enclosures with Joule heating*, J. Sci Res. 1 (3), pp. 461-472.

Rahman, M.M., Mamun M.A.H., Saidur, R., and Nagata Shuichi (2009a). *Effect Of a Heat Conducting Horizontal Circular Cylinder on MHD Mixed Convection in A Lid- Driven Enclosures Along With Joule Heating*, Int. J. of Mechanical and Materials Eng. (IJMME), Vol. 4, No. 3, pp.256-265.

Reddy J.N. (1985). *An Introduction to the Finite Element Method*, McGraw-Hill, New York, 1985.

Rudraiah, N., Barron, R. M. (1995b). *Venkatachalappa, M., and Subbaraya, C. K., "Effect of magnetic field on free convection in a rectangular enclosure*, Int. J. Engng. Sci., Vol. 33, pp. 1075-1084.

Rudraiah, N., Venkatachalappa, M., and Subbaraya, C. K. (1995a), *Combined surface tension and buoyancy-driven convection in a rectangular open enclosures in the presence of magnetic field*, Int. J. Non-linear Mech., Vol. 30(5), pp. 759-770.

Singh, S., and Sharif, M. A. R. (2003). *Mixed convective cooling of a rectangular cavity with inlet and exit openings on differentially heated side walls*, Numer. Heat Transfer, Part A Vol. 44, pp. 233–253.

Taylor C. and Hood P. (1973). *Computer and Fluids*, **1** (1), 73 .http://dx.doi.org/10.1016/0045-7930(73)90027-3

.